

Change-over of carrier type and magneto-transport property in Cu doped Bi_2Te_3 Topological Insulators

Abhishek Singh¹, Rahul Singh¹, A. Lakhani², T. Patel², G. S. Okram², V. Ganeshan², A. K. Ghosh³ and Sandip Chatterjee^{1,*}

¹)Department of Physics, Indian Institute of Technology (Banaras Hindu University), Varanasi-221005, India

²)UGC-DAE Consortium for Scientific Research, Indore, Madhya Pradesh 452001, India

³)Department of Physics, Banaras Hindu University, Varanasi-221005, India

Abstract

Structural, resistivity, thermoelectric power and magneto-transport properties of Cu doped Bi_2Te_3 topological insulators have been investigated. The occurrence of the tuning of charge carriers from n type to p type by Cu doping at Te sites of Bi_2Te_3 is observed both from Hall effect and thermoelectric power measurements. Carrier mobility decreases with the doping of Cu which provides evidence of the movement of Fermi level from bulk conduction band to the bulk valence band. Thermoelectric power also increases with doping of Cu. Moreover linear magnetoresistance (LMR) has been observed at high magnetic field in pure Bi_2Te_3 which is associated to the gapless topological surface states protected by time reversal symmetry (TRS), whereas doping of Cu breaks TRS and an opening of band gap occurs which quenches the LMR.

Topological insulators (TIs) are a new class of materials, which are insulating in bulk but conducting at the surface. This is due to the gapless edge or spin resolved surface states (SS), which are topologically protected by time reversal symmetry. The spins are locked in the perpendicular direction of momentum due to the strong spin-orbit interaction. As a matter of fact, electrical conduction is robust against backscattering at the edge states or on the surfaces in TIs. These special helical spin properties of electrons make TIs interesting and relevant for new physics. Since the locking of spin and orbital states is protected by time reversal symmetry,¹ the delocalized surface states are unaffected from nonmagnetic dopants and defects. The possibility of Majorana Fermions,² topological superconductivity,^{3,4} novel magnetoelectric quantum states,⁵ the absence of backscattering from nonmagnetic impurities,⁶ exciton condensation,⁷ magnetic monopole,⁸ and anomalous quantum Hall effect⁹ types of exotic properties in TIs are very promising in the application of spintronic devices and quantum computing. Topological surface states in Bi_2Te_3 and Bi_2Se_3 with only one massless Dirac cone on each surface have been studied using Angle-resolved photoemission spectroscopy (ARPES).^{10,11} Quantum magneto-transport phenomenon such as weak antilocalization,¹²⁻¹⁴ Aharonov-Bohm oscillations,¹⁵ and quantum conductance fluctuations,¹⁶ are associated with surface states. The time reversal symmetry protection of the Dirac point can be lifted by magnetic dopants, resulting in a band gap due to the separation in the upper and lower branches of the Dirac cone.¹⁷

Moreover, materials with large magneto resistance (MR) have been of great interest from the application point of view as well as for fundamental research. According to Abrikosov's theory,¹⁸ a quantum linear magneto resistance which is ideal for application, is expected in the materials having zero band gap with linear energy spectrum. Materials with linear MR might be used in magneto electronic applications such as multifunctional electromagnetic application and disc reading heads. Recently, a giant and linear MR in TIs have been reported.¹⁹⁻²⁶ Zhang et al. showed that on ultra thin film of Bi_2Se_3 a surface state gap opened at the Dirac point because of tunnelling between the top and bottom surface states.²⁷ Interestingly, while most of the reports in Bi_2Te_3 samples were on doping on Bi site,²⁸⁻³² doping on Te site has not yet been reported to the best of our knowledge, which however might be equally interesting to study. Here we report a study of 5% Cu doping on Te site in Bi_2Te_3 . It is observed from Hall resistivity and thermoelectric data that type of carrier changes from n type to

p type with Cu doping. Also the magneto resistance changes from linear to non-linear behavior on doping.

Single crystals of $\text{Bi}_2\text{Cu}_x\text{Te}_{3-x}$ ($x=0, 0.15$) were grown by modified Bridgman method. High purity powder of Bi (99.999%), Te(99.999%) and Cu (99.999%) were mixed uniformly in their stoichiometric ratios. The mixture was sealed in quartz tube after evacuating down to $\sim 10^{-6}$ torr. The crystal growth involves cooling from 950°C to 550°C in a period of 24 hours and then annealing at this temperature for 72 hours. Silver coloured single crystals were then cooled down to room temperature slowly. The transport properties were measured by using the physical property measurement system (PPMS) from Quantum Design. Thermopower was measured using a standard home-made set up. Sample was sandwiched between two cylindrical oxygen-free highly conducting copper blocks in vacuum. The voltage difference between the cold and the hot ends was measured at each chosen temperature (details are given in Ref. 33).

Single crystals of $\text{Bi}_2\text{Cu}_x\text{Te}_{3-x}$ ($x=0, 0.15$) with the cleaved surface along the basal planes were characterized using X-ray diffraction method collected at room temperature [Fig. 1(a) and (b)]. X-ray diffracted beam directions showed only the (00L) with space group R-3m. The Full Width Half Maxima (FWHM) of the (003) peak is 0.115° and 0.125° whereas for (006) peak it is 0.131° and 0.137° for undoped and doped samples respectively which are very small indicating that as prepared samples have excellent single crystallinity in long range. Around $2\theta=54^\circ$ and 64° , a small splitting due to the difference in the wavelength of X-ray source of CuK_α and CuK_β radiation is observed. An additional peak around $2\theta=40^\circ$ for both the samples is observed which might be due to the slight misalignment or slight tilt angle of the crystallinity of as cleaved single crystals.

In order to see the electrical transport behaviour of the materials, temperature variation of resistivity under zero magnetic field for pure and Cu doped Bi_2Te_3 samples were carried out [Fig. 2(a)]. It is observed that the resistivity increases with temperature indicating typical metallic behaviour. Resistivity of doped sample is almost four times higher than that of the undoped sample which might be attributed to the mixture of bulk valence band and topological surface state.³⁴ The presence of wiggles in the resistivity data of Cu doped samples also confirms this indicating that bulk state is becoming significant above a critical temperature. Figure 2(b) shows the variation of Seebeck coefficient with temperature for both the Bi_2Te_3 and $\text{Bi}_2\text{Cu}_{0.15}\text{Te}_{2.85}$ samples in the temperature range of 10K-300K. Seebeck coefficient for pure

Bi₂Te₃ sample shows negative slope whereas Bi₂Cu_{0.15}Te_{2.85} sample shows positive slope in the whole range of temperature, which indicates that a change-over from *n* type conduction to *p* type conduction occurs with Cu doping in Bi₂Te₃. Moreover the maximum absolute value of Seebeck coefficient in case of Bi₂Te₃ is 142.8 μV/K whereas in doped sample it is around 159.8 μV/K. The values are consistent with those reported by Cao et.al.³⁵ Recently Seebeck coefficient of Bi₂Te₃/Cu composite has been reported.³⁶ It is observed as the Cu content increases the value of the Seebeck coefficient increases but it remains negative.³⁶ In the present investigation doping of Cu is not only tuning the carrier type but also increasing absolute value of Seebeck coefficient. To determine the efficiency of thermoelectric power we have calculated the power factor [shown in the inset of Fig.2(b)] of pure and undoped samples using the formula

$$\text{Power factor} = S^2/\rho$$

Where ρ is the electrical resistivity and S is the Seebeck coefficient. It has already been shown that with increase of the temperature electrical resistivity increases in both pure and doped samples but the increase in Seebeck coefficient (S) is much larger than the increase of electrical resistivity which gives rise to the increase of power factor with increasing temperature.

In order to determine the carrier concentration (*n* or *p*) and mobility (μ) of the pure and Cu doped Bi₂Te₃, we have also carried out the Hall measurement at 200K and 300K. The type of carrier we have determined first and then the carrier concentration has been calculated using the slope of the Hall resistivity. Using the data of carrier concentration and electrical resistivity we determined carrier mobility of the samples. Fig.3(a) shows the variation of Hall resistivity as a function of applied magnetic fields at temperatures 200 and 300K for pure Bi₂Te₃. Slope of the curve is negative which shows that carriers in pure Bi₂Te₃ are *n* type for the entire range of temperature of measurement which is also consistent with the negative Seebeck coefficient of the sample.

Calculated carrier concentration (*n*) of the pure Bi₂Te₃ is shown in the inset 1 of Fig. 3(a) which comes in the range of reported value given by Zhang et.al.³⁷ Since topological insulators are insulating in bulk but conducting on surface, it might be that at high temperature bulk contribution is dominating over surface contribution of the sample. As we know topological surface state is a complete quantum phenomenon, existence of quantum mechanical behavior is significant at very low temperature. As a matter of fact, at very low temperature surface state is

dominating over bulk state and that is why the increment in carrier concentration is very low at low temperature ($T \leq 20\text{K}$) whereas it is very high at high temperature. Moreover, the rate of increment of carrier density is also increasing with the increase of temperature, this also confirms that bulk insulating character is dominating over surface metallic character of the sample.

We have also calculated the mobility (μ) of the carriers from the Hall data. Calculated mobility as function of temperature (without Field) has been shown in the inset2 of Fig.3(a). Mobility for pure Bi_2Te_3 sample at the applied field 2T is $271.48\text{cm}^2/\text{Vsec}$ and $131.68\text{cm}^2/\text{Vsec}$ at 200K and 300K respectively whereas at Field 5T it is $225.99\text{cm}^2/\text{Vsec}$ and $126.71\text{cm}^2/\text{Vsec}$ at 200K and 300K respectively. Hence it is clear that as we increase both the temperature and field, mobility decreases. This is as expected because with decreasing temperature, freezing out of phonons takes place and as a consequence, the carrier scattering and thus thermal vibration or the contribution of phonon decreases and high mobility prevails. Similar trends happen with the magnetic field.

Figure 3(b) shows the variation of Hall resistivity with the applied magnetic field for $\text{Bi}_2\text{Cu}_{0.15}\text{Te}_{2.85}$ sample at 200K and 300K. The slope of the curve is positive which indicates that carriers are p type. The carrier concentration is 2.20×10^{19} per cm^3 and 2.96×10^{19} per cm^3 at 200K and 300K, respectively. Carrier density increases with temperature similar to the undoped sample. The variation of mobility with the applied field is shown in the inset of fig.3(b). Mobility decreases with increase in field and temperature as is observed in the Bi_2Te_3 and the value is lower in $\text{Bi}_2\text{Cu}_{0.15}\text{Te}_{2.85}$ than that of the undoped sample. It may be due to the generation of electrons by Te_{Bi} antisite defects in pure sample where Fermi level lies in the conduction band. In fact, charge carriers are in conduction band and exert less resistivity in comparison to valence band and hence the mobility will be high. Doping of Cu drives the Fermi level into valence band leading to p type behavior and as the charge carriers are in valence band, more resistance (one order higher than that of pure sample) and less mobility are observed than those in conduction band which is also clear from the resistivity data [Fig. 2(a)]. It is worthwhile to mention that the presence of foreign element i.e. Cu may also produce extra center of scattering and result in higher resistivity as is observed in Fig. 2. Moreover, number of charge carriers, calculated from the Hall measurement in pure sample, is higher than that of doped one giving rise to the low resistivity. Therefore, both Hall data and thermopower data corroborate the resistivity data.

Variation in percentage of magneto resistance (MR) as a function of applied magnetic field under different temperatures for undoped and doped samples is shown in Fig. 4(a) and 4(b), respectively. Fig. 4 (a) shows a clear linear and non-saturating MR of Bi_2Te_3 . MR is increasing with applied field but decreasing with increasing temperature. As it is clear from Hall data that as we increase temperature, carrier concentration (n_0) increases and MR decreases. Similarly with increasing applied field (H), MR increases [Fig. 4(a)]. No saturation has been seen in pure sample whereas saturation has been observed in doped sample [Fig. 4 (b)]. Moreover; the %MR in undoped sample is one order higher than that of doped one. Li et al. observed that when thickness of Bi_2Te_3 thin films is greater than 2QL (quintuple layer) then topological surface state (TSS) appears.³⁸ He et al. reported that in Bi_2Se_3 thin films of thickness $< 6\text{nm}$, grown by molecular beam epitaxial method, linear magnetoresistance disappears due to opening of gap in the surface state as induced by the interface coupling.³⁹ In Bi_2Te_3 nanoplates having a thickness less than 5nm, absence of surface gapless state is observed by Kong et al.⁴⁰ In order to have a bulk band gap for the security of surface topological gapless state in Bi_2Te_3 platelike samples, thickness should be greater than 14QL. Both the doped and undoped samples have been cleaved with few mm thickness, therefore, thickness will be definitely greater than 14QL as the thickness of 1QL in Bi_2Te_3 is of the order of some nm, as a matter of fact thickness cannot be the reason for the absence of LMR in doped sample. Zhang et al.²⁷ reported that in ultrathin film of Bi_2Se_3 absence of LMR has been observed because of opening of surface state gap at the Dirac point due to the tunneling between top to bottom surface states. Tuning of band gap and changing in Hall resistivity has been observed by Lee⁴¹ in silver chalcogenides by using hydrostatic pressure. Hence, presence of LMR is possible when pressure induces closing of band gap. This shows that very small or zero band gap is essential condition for the presence of LMR. As a matter of fact the LMR is due to the presence of surface state as already reported in bulk Bi_2Te_3 .⁴² As Cu produces internal magnetic impurity i.e. magnetic field, therefore, doping of Cu changes the gapless energy spectrum into a gap. Hence, energy spectrum does not remain linear so that disappearance of LMR occurs and saturation of MR can be seen.

In conclusion, we have investigated the structural, transport and magnetotransport properties of Cu doped and undoped Bi_2Te_3 topological insulators. With Cu doping, resistivity increases as Fermi level is shifted into valence band with extra scattering centers. It is also observed that Cu doping tunes the carrier from n to p type, which is attributed to the presence of Te_{Bi} and

Bi_{Te}antisites. The observed LMR in Bi₂Te₃ single crystal is believed to be of quantum origin and associated with gapless linear energy spectrum of surface Dirac Fermions. The absence of linear magneto resistance in Cu doped sample reveals the gap opening due to the presence of magnetic impurity.

Acknowledgement

The authors are grateful to UGC-DAE Consortium for Scientific Research, Indore, India for providing facility. Authors are also grateful to CIFC, IIT(BHU) for providing facility for magnetic measurement. Authors also acknowledge Dr. Devendra Kumar for his help in the measurement.

References:

*corresponding author e-mail id: schatterji.app@iitbhu.ac.in

1. M. Z. Hasan and C. L. Kane, Rev. Mod. Phys., 82, 3045 (2010)
2. L. Fu and C.L. Kane, Phys. Rev. Lett. 102, 216403 (2009)
3. L. A. Wray, S.-Y. Xu, Y. Xia, Y. S. Hor, D. Qian, A. V. Fedorov, H. Lin, A. Bansil, R. J. Cava, and M. Z. Hasan, Nature Phys. 6, 855 (2010)
4. Y. S. Hor, A. J. Williams, J. G. Checkelsky, P. Roushan, J. Seo, Q. Xu, H. W. Zandbergen, A. Yazdani, N. P. Ong, and R. J. Cava, Phys. Rev. Lett. 104, 057001 (2010)
5. X. L. Qi and S. C. Zhang, Rev. Mod. Phys. 83, 1057 (2011)
6. P. Roushan, J. Seo, C. V. Parker, Y. S. Hor, D. Hsieh, D. Qian, A. Richardella, M. Z. Hasan, R. J. Cava, and A. Yazdani, Nature (London) 460, 1106 (2009)
7. B. Seradjeh, J.E. Moore and M. Franz, Phys. Rev. Lett. 103, 066402 (2009)
8. X.-L. Qi, R. Li, J. Zhang, and S.-C. Zhang, Science 323, 1184(2009)
9. R. Yu, W. Zhang, H.-J. Zhang, S.-C. Zhang, X. Dai, and Z. Fang, Science 329, 61, (2010).
10. Y. L. Chen, J. G. Analytis, J.-H. Chu, Z. K. Liu, S.-K. Mo, X. L. Qi, H. J. Zhang, D.H. Lu, X. Dai, Z. Fang, S. C. Zhang, I. R. Fisher, Z. Hussain, and Z.-X. Shen, Science 325, 178 (2009)

11. Y. Xia, D. Qian, D. Hsieh, L. Wary, A. Pal, H. Lin, A. Bansil, D. Grauer, Y. S. Hor, R. J. Cava, and M. Z. Hasan, *Nat. Phys.* 5, 398 (2009)
12. J. G. Checkelsky, Y. S. Hor, R. J. Cava, and N. P. Ong, *Phys. Rev. Lett.* 106, 196801 (2011)
13. H. T. He, G. Wang, T. Zhang, I. K. Sou, G. K. L. Wong, J. N. Wang, H. Z. Lu, S. Q. Shen, and F. C. Zhang, *Phys. Rev. Lett.* 106, 166805 (2011)
14. J. Chen, H. J. Qin, F. Yang, J. Liu, T. Guan, F. M. Qu, G. H. Zhang, J. R. Shi, X. C. Xie, C. L. Yang, K. H. Wu, Y. Q. Li, and L. Lu, *Phys. Rev. Lett.* 105, 176602 (2010)
15. H. L. Peng, K. J. Lai, D. S. Kong, S. Meister, Y. L. Chen, X. L. Qi, S. C. Zhang, Z. X. Shen, and Y. Cui, *Nature Mater.* 9, 225 (2010)
16. J. G. Checkelsky, Y. S. Hor, M.-H. Liu, D.-X. Qu, R. J. Cava, and N. P. Ong, *Phys. Rev. Lett.* 103, 246601 (2009)
17. Y. L. Chen, J.-H. Chu, J. G. Analytis, Z. K. Liu, K. Igarashi, H.-H. Kuo, X. L. Qi, S. K. Mo, R. G. Moore, D. H. Lu, M. Hashimoto, T. Sasagawa, S. C. Zhang, I. R. Fisher, Z. Hussain, Z. X. Shen, *Science* 329, 659 (2010)
18. Abrikosov, A. A. *Phys. Rev. B* 58, 2788(1998)
19. H. Tang, D. Liang, R. L. J. Qiu, and X. P. A. Gao, *ACS Nano* 5, 7510 (2011).
20. B. F. Gao, P. Gehring, M. Burghard, and K. Kern, *Appl. Phys. Lett.* 100, 212402 (2012).
21. X. Y. He, T. Guan, X. X. Wang, B. J. Feng, P. Cheng, L. Chen, Y. Q. Li, and K. H. Wu, *Appl. Phys. Lett.* 101, 123111 (2012)
22. X. L. Wang, Y. Du, S. X. Dou, and C. Zhang, *Phys. Rev. Lett.* 108, 266806 (2012)
23. H. B. Zhang, H. L. Yu, D. H. Bao, S. W. Li, C. X. Wang, and G. W. Yang, *Phys. Rev. B* 86, 075102 (2012)
24. Z. J. Yue, X. L. Wang, and S. X. Dou, *Appl. Phys. Lett.* 101, 152107 (2012)
25. S. X. Zhang, R. D. McDonald, R. Shekhter, Z. X. Bi, Y. Li, Q. X. Jia, and S. T. Picraux, *Appl. Phys. Lett.* 101, 202403 (2012)
26. B. A. Assaf, T. Gardinal, P. Wei, F. Katmis, J. S. Moodera, and D. Heiman, *Appl. Phys. Lett.* 102, 012102 (2013)

27. Y. Zhang, K. He, C. Z. Chang, C. L. Song, L. L. Wang, X. Chen, J. F. Jia, Z. Fang, X. Dai, W. Y. Shan, S. Q. Shen, Q. Niu, X. L. Qi, S. C. Zhang, X. C. Ma, and Q. K. Xue, *Nat. Phys.* 6, 584 (2010)
28. M. D. Watson, L. J. Collins-McIntyre, L. R. Shelford, A. I. Coldea, D. Prabhakaran, S. C. Speller, T. Mousavi, C. R. M. Grovenor, Z. Salman, S. R. Giblin, G. van der Laan and T. Hesjedal, *New Journal of Physics* 15, 103016(2013)
29. Y. S. Hor, P. Roushan, H. Beidenkopf, J. Seo, D. Qu, J. G. Checkelsky, L. A. Wray, D. Hsieh, Y. Xia, S.-Y. Xu, D. Qian, M. Z. Hasan, N. P. Ong, A. Yazdani, and R. J. Cava, *Phys. Rev. B* 81, 195203, (2010)
30. X. F. Kou, W. J. Jiang, M. R. Lang, F. X. Xiu, L. He, Y. Wang, Y. Wang, X. X. Yu, A. V. Fedorov, P. Zhang, and K. L. Wang, *J. Appl. Phys.* 112, 063912 (2012)
31. H. Chi, W. Liu, K. Sun, X. Su, G. Wang, P. Lošt'ák, V. Kucek, Č. Drašar, and C. Uher, *Phys. Rev. B* 88, 045202(2013)
32. J. S. Dyck, P. Hájek, P. Lošt'ák, and C. Uher, *Phys. Rev. B* 65, 115212,(2002)
33. A. Soni and G. S. Okram *Rev. Sci. Instrum.* 79, 125103 (2008)
34. N. H. Jo, K. J. Lee, C. M. Kim, K. Okamoto, A. Kimura, K. Miyamoto, T. Okuda, Y. K. Kim, Z. Lee, T. Onimaru, T. Takabatake, M. H. Jung, *Phys. Rev. B* 87, 201105 (2013)
35. H. Cao, R. Venkatasubramanian, C. Liu, J. Pierce, H. Yang, M. Z. Hasan, Y. Wu, and Y. P. Chen, *Appl. Phys. Lett.* 101, 162104 (2012)
36. F.R. SIE, C.H. KUO, C.S. HWANG, Y.W. CHOU, C.H. YEH, Y.L. LIN, and J.Y. HUANG, *J. Elec. Mater.* 45, 1927 (2016)
37. S. J. Zhang, J. L. Zhang, X. H. Yu, J. Zhu, P. P. Kong, S. M. Feng, Q. Q. Liu, L. X. Yang, X. C. Wang, L. Z. Cao, W. G. Yang, L. Wang, H. K. Mao, Y. S. Zhao, H. Z. Liu, X. Dai, Z. Fang, S. C. Zhang, and C. Q. Jin, *J. Appl. Phys.* 111, 112630 (2012)
38. Y. Y. Li, G. Wang, X. G. Zhu, M. H. Liu, C. Ye, X. Chen, Y. Y. Wang, K. He, L. L. Wang, X. C. Ma, H. J. Zhang, X. Dai, Z. Fang, X. C. Xie, Y. Liu, X. L. Qi, J. F. Jia, S. C. Zhang and Q. K. Xue, *Adv. Mater.* 22,4002(2010)

39. H. He, B. Li, H. Liu, X. Guo, Z. Wang, M. Xie, and J. Wang, *Appl. Phys. Lett.* 100, 032105 (2012)
40. D. Kong, Y. Chen, J. J. Cha, Q. Zhang, J. G. Analytis, K. Lai, Z. Liu, S. S. Hong, K. J. Koski, S. K. Mo, Z. Hussain, I. R. Fisher, Z.-X. She and Y. Cui, *Nature Nanotechnology* 6, 705 (2011)
41. M. Lee, T. F. Rosenbaum, M. L. Saboungi, and H. S. Schnyders, *Phys. Rev. Lett.* 88, 066602 (2002)
42. S. Barua, K P Rajeev and A. K Gupta, *J. Phys. Condens. Matter* 27, 015601 (2015)

Figure Captions:

Fig1. Room temperature X-ray diffraction patterns of (a) Bi_2Te_3 and (b) $\text{Bi}_2\text{Cu}_{0.15}\text{Te}_{2.85}$ single crystals.

Fig2. (a) Temperature dependence of electrical resistivity for Bi_2Te_3 and $\text{Bi}_2\text{Cu}_{0.15}\text{Te}_{2.85}$ single crystals showing metallic behavior and (b) Variation of Seebeck coefficient as a function of temperature. Inset represents the power factor (PF) of the Bi_2Te_3 and $\text{Bi}_2\text{Cu}_{0.15}\text{Te}_{2.85}$ single crystals.

Fig3. (a) Magnetic field dependence of the Hall resistivity of the pure Bi_2Te_3 single crystal at 200K and 300K. Inset1 represents the variation of 3D carrier concentration as a function of temperature whereas Inset 2 shows the variation of carrier mobility with temperature for the undoped Bi_2Te_3 and (b) Magnetic field dependence of the Hall resistivity of the $\text{Bi}_2\text{Cu}_{0.15}\text{Te}_{2.85}$ single crystal at 200K and 300K, the inset in fig is the carrier mobility as a function of applied magnetic field at 200K and 300K.

Fig4. (a) Normalized magnetoresistance $\frac{R(H)-R(0)}{R(0)}$ as a function of magnetic field for Bi_2Te_3 at different temperatures showing linear behavior and (b) Normalized magnetoresistance $\frac{R(H)-R(0)}{R(0)}$ as a function of magnetic field for $\text{Bi}_2\text{Cu}_{0.15}\text{Te}_{2.85}$ at different temperatures showing saturating behavior.

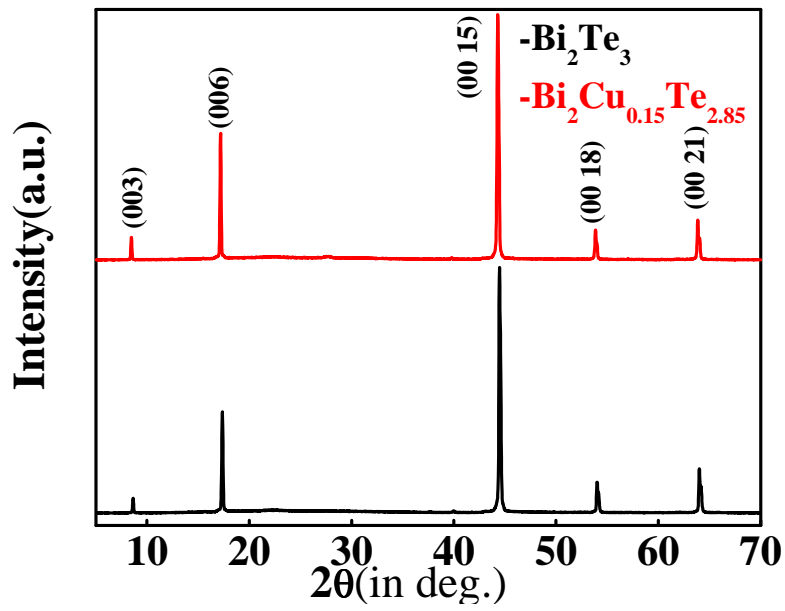
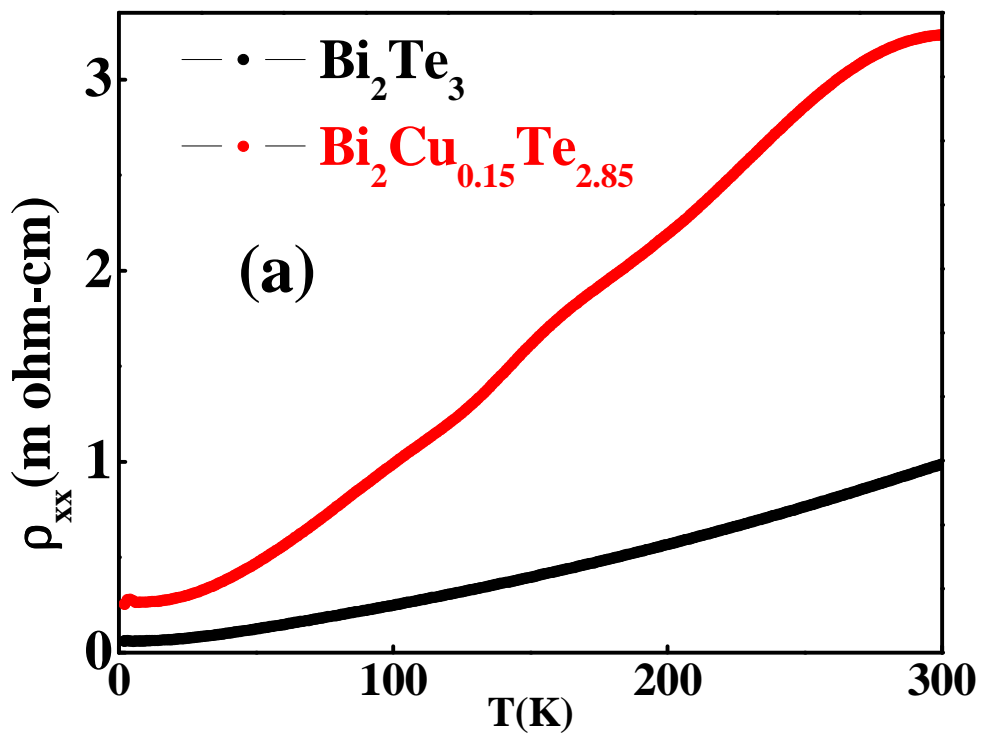


Fig1



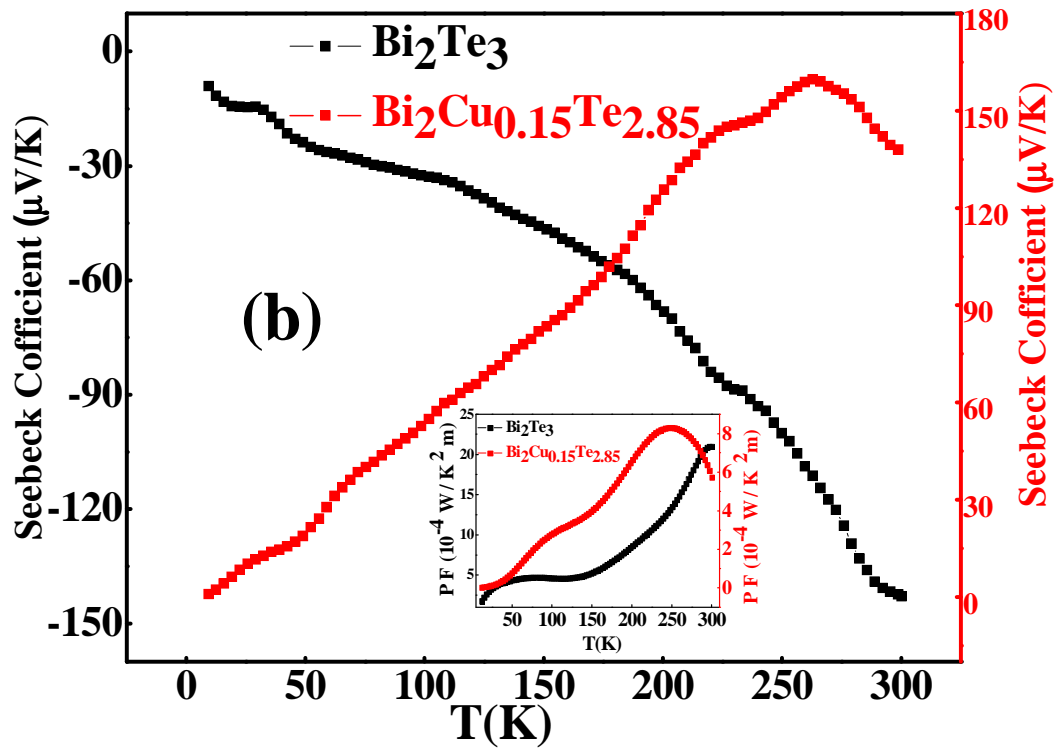
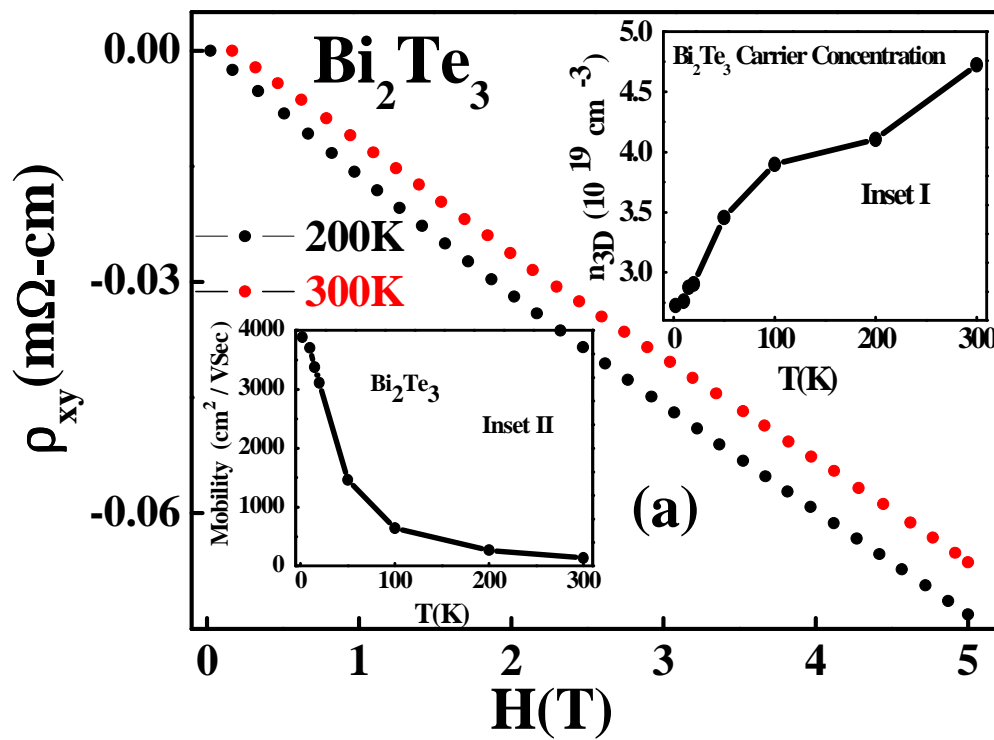


Fig2



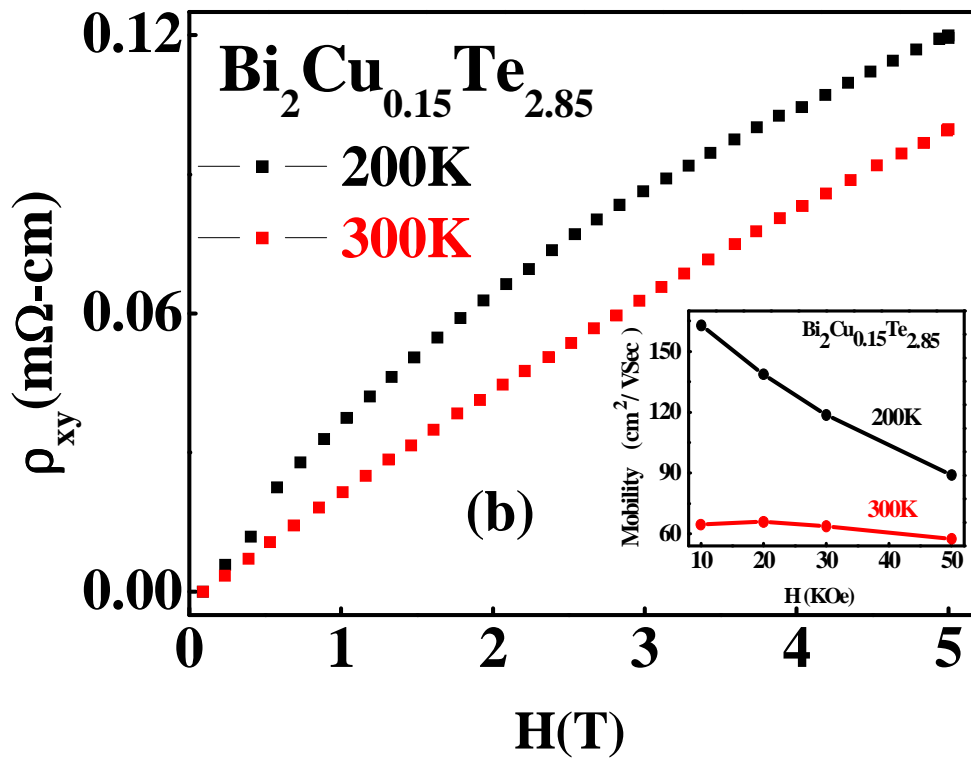


Fig3

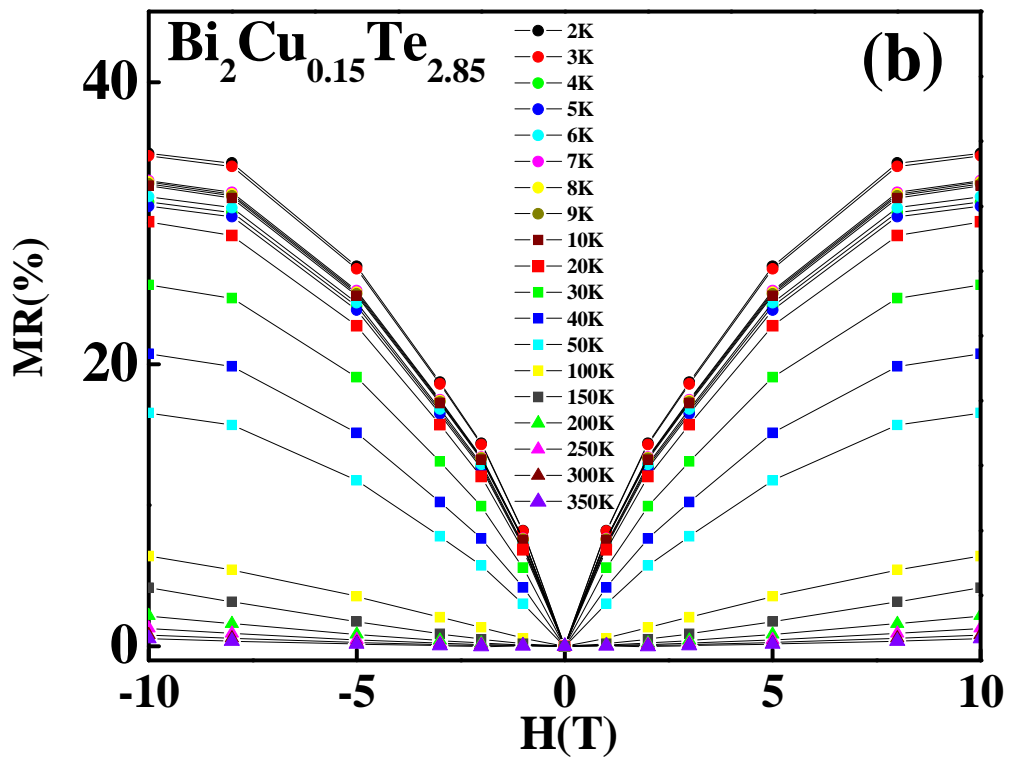
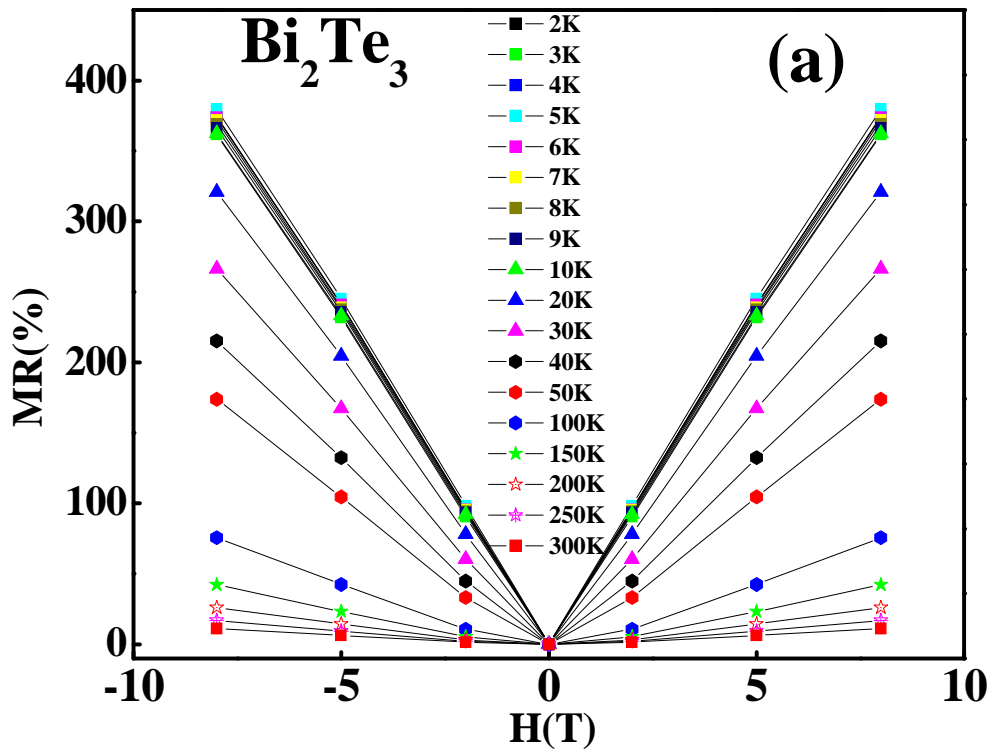


Fig4